RESEARCH PAPER

Acta Neurobiol Exp 2025, 85: 176–186
DOI: 10.55782/1zwmve34

Lack of unconventional myosin VI is associated with brain enlargement and gliosis progressing with age

Jolanta Nowak[1], Justyna Karolczak[1,2], Henryk Bilski[3], Serge Weis[2], Maria Jolanta Rędowicz[1]*

[1] Laboratory of Molecular Basis of Cell Motility, Nencki Institute of Experimental Biology, Polish Academy of Sciences, Warsaw, Poland
[2] Division of Neuropathology, Department of Pathology and Molecular Pathology, Neuromed Campus, Kepler University Hospital, Johannes Kepler University, Linz, Austria and Clinical Research Institute for Neurosciences, Johannes Kepler University, Linz, Austria
[3] Laboratory of Electron Microscopy, Nencki Institute of Experimental Biology, Polish Academy of Sciences, Warsaw, Poland
** Email: j.redowicz@nencki.edu.pl*

Myosin VI (MVI) is a unique unconventional myosin which, unlike other myosins, moves towards the minus end of actin filaments. It is involved in numerous cellular processes such as endocytosis and trafficking, cell migration and adhesion, and gene transcription. It is widely expressed in all tissues, including the brain. Its lack in adult murine brains is associated with gliosis and impairment of neuronal transmission. Here, we demonstrate that the MVI level in the total mouse brain and its regions (cerebral cortex, cerebellum, and hippocampus) increases with the animal's age (from newborn up to 12-month-old mice). Its lack leads to enlargement of the brain and its examined areas, and an increase of the level of GFAP, the marker of glia cells, in adult mice. The data indicate an involvement of MVI in the brain maturation and possibly in development of an age-dependent gliosis.

Key words: brain, GFAP, gliosis, myosin VI, vimentin

INTRODUCTION

Myosins are actin-based molecular motors, originally discovered in skeletal muscles, forming a structurally and functionally diverse superfamily that consists of more than 35 distinct families (Odronitz & Kollmar, 2007). The myosin classification is based on the diversity of amino acid sequences of the N-terminal motor domain (containing the ATP- and actin-binding sites) responsible for myosin motor activity. Myosins are expressed across *Eukaryota,* and the number of their isoforms is associated with evolutionary development. In humans, there are 40 myosin encoding genes, which belong to 12 families (Berg et al., 2001). Those myosins which are able to form filaments (mainly muscle isoforms) are designated as conventional, while all others are named as unconventional. Myosins are involved in nearly all cellular processes, ranging from muscle contraction and cell motility to endocytosis and transcription; mutations or changes in their expression cause numerous pathologies (Redowicz, 2002).

Unconventional myosin VI (MVI) is a unique motor that, unlike other known myosins, moves towards the minus end of the actin filament (Wells et al., 1999; Nishikawa et al., 2002). The MVI 140-kDa heavy chain is aligned in the classical myosin domain pattern: N-terminal motor domain, a neck (with one classical IQ motif to which calmodulin binds), and a tail domain. The C-terminal part of the tail forms a globular domain, which is essential for cargo binding and/or interaction with binding partners as well as with PIP_2-containing liposomes (Sweeney & Houdusse, 2007; 2010; Chibalina et al., 2009). In humans, MVI is encoded by a single gene *(MYO6)*, which is expressed in most of the tissues, including the central nervous system (Avraham et al., 1997). The data gathered so far indicate that MVI is engaged in endocytosis and intracellular transport of

Received 13 November 2025, accepted 19 December 2025

vesicles and organelles, actin cytoskeleton organization, cell migration, maintenance of the Golgi apparatus, mitophagy, and gene transcription and nucleolar maintenance (Kruppa et al., 2018; Magistrati & Polo, 2021; Hari-Gupta et al., 2022; Nowak et al., 2024). MVI has been shown to be involved in functions of the central nervous system (CNS) (Suter et al., 2000; Osterweil et al., 2005; Yano et al., 2006, Lewis et al., 2011; Nash et al., 2010; Wagner et al., 2019). In adult murine brains, MVI is present in many layers of the cerebral cortex, hippocampus and cerebellum (Osterweil et al., 2005; Wagner et al., 2019). On the subcellular level it is present in the perinuclear region, and in dendrites where it localizes to postsynaptic densities (Suter et al., 2000; Osterweil et al., 2005; Yano et al., 2006). Most of the functional studies have been performed on adult brains and primary neuronal cultures obtained from natural MVI knockout mice (Snell's waltzer, SV, MVI-KO), exhibiting hyperactivity due to vestibular defects (Deol & Green 1966). Lack of MVI manifests with a decrease in the synapse number, abnormally short dendritic spines, as well as a significant deficit in the stimulation-induced internalization of glutamate receptors. As a consequence, these aberrations lead to impaired basal synaptic transmission (Osterweil et al., 2005; Yano et al., 2006; Nash et al., 2010). Also, profound gliosis associated with the brain enlargement has been observed in SV brains (Osterweil et al., 2005). A search for mechanisms behind these observations revealed that MVI in complex with adaptor protein GIPC1 is necessary for BDNF-TrkB-mediated facilitation of long-term potentiation in hippocampal neurons (Yano et al., 2006). Besides GIPC-1, several other MVI partners have been identified, which are important for neuronal processes such as DOCK7 (dedicator of cytokinesis 7), SAP97, and TLS (translated in sarcoma) (Wu et al., 2002; Takarada et al., 2009; Majewski et al., 2012).

MVI has also been shown to be involved in a dynamic remodeling of ribosomes and endoplasmic reticulum in nerve termini, in tuning dendrite arbor subdivision as well as in the localization of axonal proteins (Lewis et al., 2011; Zheng et al., 2015; Yoong et al., 2020; Deng et al., 2021). Furthermore, there are reports linking MVI with brain pathologies including brain injuries, Alzheimer's disease, and amyotrophic lateral sclerosis (Feuillette et al., 2010; Karolczak et al., 2013; Sundaramoorthy et al., 2015; Makioka et al., 2016; Deng et al., 2021; Lee et al., 2024).

While there are several reports on MVI functions in the CNS, very little is known about its involvement in brain development and growth. It has been shown that its level in dorsal root ganglion (DRG) neurons is increasing during embryonic development (Suter et al., 2000). Osterweil et al. (2005) revealed that the MVI level in the mouse brain does not change between newborns and young adults. However, there are no further studies addressing whether and how the MVI level is changing with mouse maturation. Also, it is not known when the MVI-associated brain enlargement and gliosis develop, as well as whether these changes apply to all brain regions.

To address these problems, we examined the effects of lack of MVI on the weight of the brain and its regions (i.e., cerebral cortex, hippocampus, and cerebellum) as well as on the level of glial fibrillary protein (GFAP), the gliosis marker, during the tested lifespan (i.e., in newborns, 3-month-old, and 12-month-old mice). Also, we checked in control (i.e., heterozygous) mice whether the level of MVI changes with age and varies between the particular brain regions.

METHODS

Animals

Snell's waltzer (SV) mice, maintained on a C57BL/6J genetic background, were used in the study. This strain carries a spontaneous mutation in the *Myo6* gene, originally identified at The Jackson Laboratory (Deol & Green, 1966). The mutation consists of a 130-base pair deletion introducing a premature stop codon in the MVI neck region, leading to a lack of functional MVI. SV mice serve as a natural knockout model for MVI. To examine the role of MVI in the brain, we performed analyses on the whole brain and its regions (i.e., cerebral cortex, hippocampus, and cerebellum) derived from male mice at different stages of development: newborn (P0), 3- and 12-month-old (3M and 12M, respectively). This strategy allowed us to investigate the changes occurring during animal/brain maturation. The decision to use male mice in the current study was based on the numerous former reports (including ours), which were focused only on males (Avraham et al., 1997; Karatsai et al., 2023; Wojton et al., 2025). Besides, using males allowed for controlled and reproducible results while eliminating confounding variables associated with hormonal fluctuations, estrus cycles, or potential sex-specific responses. The only exception was for experiments involving newborn (P0) mice, where pup samples from both males and females were analyzed. However, we did not identify the sex in individual animals.

Each experiment was performed in at least four biological replicates (N≥4) using heterozygotes as controls (termed herein as WT) and mutant SV (termed herein as MVI-KO) mice from the same litter. The mice

were on the standard rodent chow diet and housed under pathogen-free conditions in the animal facility of the Nencki Institute. Animal housing and euthanasia procedures (mice were euthanized with a lethal dose of isoflurane followed by cervical dislocation) were performed in compliance with the European Communities Council directives adopted by the Polish Parliament (Act of January 15, 2015, on the use of animals in scientific investigations). Since all studies were conducted on isolated tissues from non-suffering animals, ethics committee approval was not required under the provisions of the abovementioned Act. Instead, all procedures were performed with the approval of the Director of the Nencki Institute of Experimental Biology. The following internal approvals were granted: 155/2020/IBD and 218/2024/IBD.

Western blot analysis

Mice's brains were weighed, and the left hemispheres were left for homogenization. Right hemispheres were dissected into cerebral cortex, cerebellum, and hippocampus, and after weighing, homogenized in 0.1 M phosphate buffer, pH 7.2, supplemented with 1 mM phenylmethanesulfonyl fluoride at a 1:50 weight-to-volume (w/v) ratio; no protein measurements were done as all the samples were standardized to the same w/v ratio. The homogenates (15 µl for all samples) were next subjected to the SDS gel electrophoresis using 12% polyacrylamide gels, and then transferred to a nitrocellulose membrane. The transfer efficiency was examined by Ponceau red staining immediately after the transfer. All the procedures were performed at room temperature. Next, the membrane was blocked for 1 h in TBS containing 3% non-fat milk powder and 0.2% Triton X-100 followed by 1-hour incubation with the polyclonal antibodies against MVI (at 1:1000 dilution, from Proteus, USA, Cat. no.: 25-6791), glial fibrillary acidic protein, GFAP (at 1:45,000 dilution, from Merck Millipore, USA, Cat. no.: ab7260) and monoclonal antibodies against vimentin (at 1:5,000 dilution, from Abcam Limited, UK, Cat. no.: ab92547) and GAPDH (at 1: 20,000 dilution, from Merck Millipore, USA, Cat. no.: MAB374). Primary antibodies were detected by the following secondary antibodies conjugated with horse radish peroxidase: anti-mouse IgG (at 1:10,000 dilution from Merck Millipore, Cat. no.: AP308P) and anti-rabbit IgG (at 1:10,000 dilution from Merck Millipore, Cat. no.: AP307P). The reaction was developed using the electrochemiluminescence (ECL) method as described by the manufacturer (Merck Millipore). Densitometric analysis was performed on the X-ray film scans using Fiji distribution of ImageJ 1.52a software (National Institutes of Health and the University of Wisconsin, USA). The intensity of bands corresponding to MVI, GFAP, vimentin, and GAPDH was assessed, and the levels of proteins of interest were normalized to the GAPDH level.

Statistical analysis

Results were expressed as means ± standard deviation (SD) or standard error of the mean (SEM) as stated in the figure legends. The number of animals was provided in the figure legends. When the data were normally distributed, we performed a parametric two-tailed Student's t-test or a one-way ANOVA test in GraphPad Prism 8.4.3 software (San Diego, CA, USA). Data that were non-normally distributed were analyzed with a non-parametric Mann-Whitney or Kruskal-Wallis tests to determine statistical significance. Statistical significance was defined as *or #p<0.05, **p<0.01, ***p<0.001, ****, p<0.0001. *, comparisons between MVI-KO and control WT counterparts at the indicated age, and #, comparisons of between 3M and 12M WT or 3M and 12M MVI-KO mice, ns – no statistical significance.

RESULTS

Lack of MVI affects the weight of the brain and its regions

To assess whether and how lack of MVI affects the mouse brain, we examined the weight of the brain (Br) and its regions: cerebral cortex (C), cerebellum (Cl), and hippocampus (H) of P0, 3M, and 12M mice (Fig. 1 A-D). The analysis revealed that the weight of the brain and its regions did not significantly differ between the samples of WT and MVI-KO mice. The exception was the weight of whole brains of 12M MVI-KO mice, which was significantly higher than their WT counterparts (Fig. 1A). It is noteworthy that we have shown in our previous report that the body weight (Bw) of the examined MVI-KO mice was significantly lower with respect to WT animals, and the mutant mice were smaller than the WT counterparts (Karatsai et al., 2023). We made the same observations for the mice examined within this study (not shown).

Evaluation of whole brain to body weight (Br/Bw) as well as of the examined regions: cerebral cortex (C/Bw), cerebellum (Cl/Bw), and hippocampus (H/Bw) ratios revealed a significant increase in examined values in adult brain samples of MVI-KO mice (Fig. 2A-D). The differences were most evident for 3M and 12M whole

brains and cerebellum, as well as for 12M cerebral cortex and hippocampus. A similar trend was observed for the whole brain, cerebral cortex (here we obtained a statistical relevance), and cerebellum of newborn mice (P0). However, for the hippocampus, the H/Bw ratio in the P0 mutant was lower than in its WT counterpart, though without statistical significance.

Next, we evaluated the ratio of the examined brain regions with regard to the whole brain weight (C/Br, Cl/Br and H/Br) to reveal whether the abovementioned differences are uniformly distributed in the brain during animal growth and maturation (Fig. 3A-C). We did not observe any significant difference in C/Br and Cl/Br values in P0, 3M, and 12M animals, as well as the H/Br ratio in 3M and 12M animals. However, we observed that the H/Br value in MVI-KO P0 brains was significantly lower with respect to the WT P0 brain (Fig. 3C).

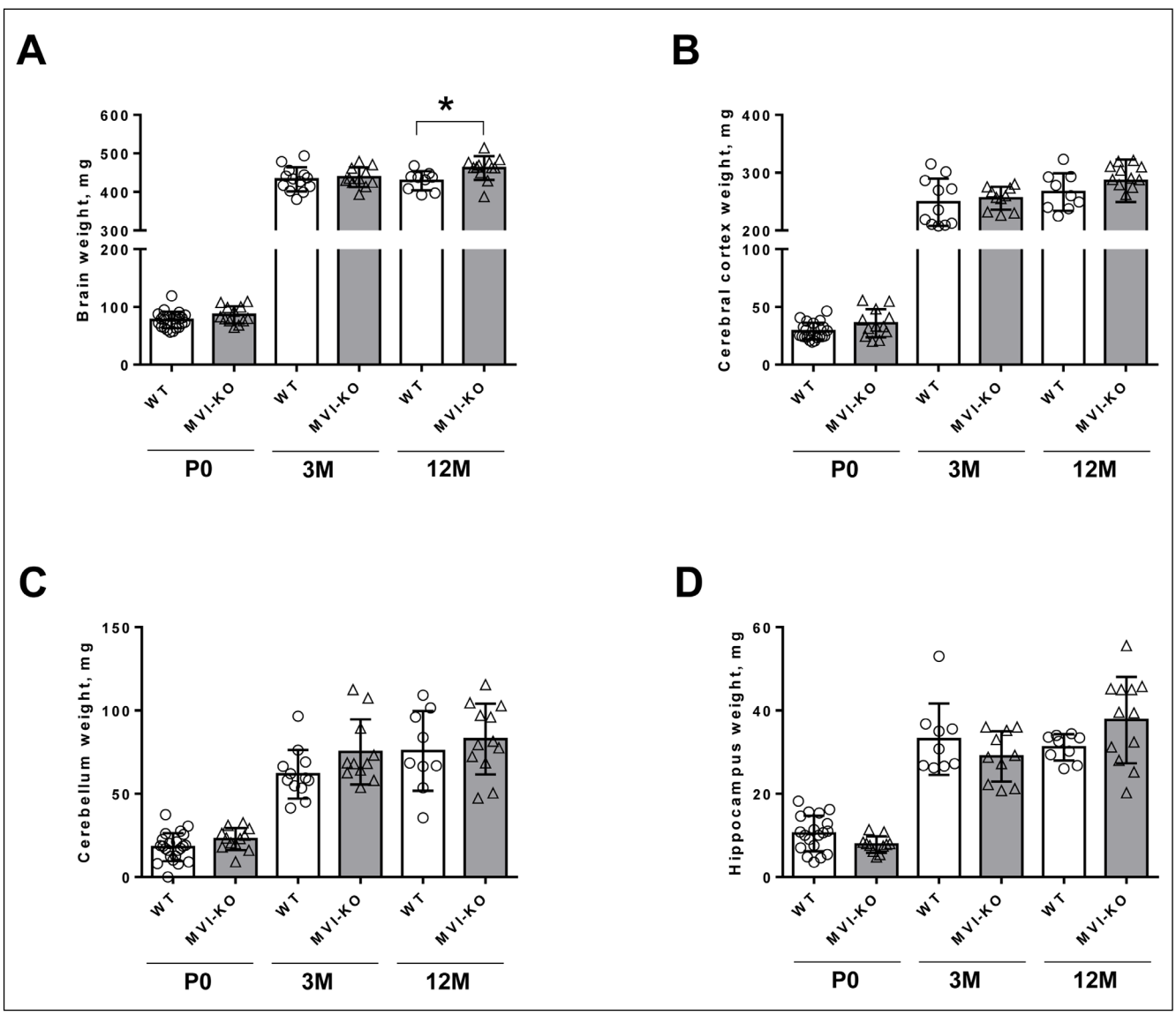

Fig. 1. Effect of lack of MVI on the weight of the brain and its regions. The weight of the total brain (A), cerebral cortex (B), cerebellum (C), and hippocampus (D) in WT and MVI-KO P0, 3M and 12M mice was assessed. The data are presented as mean ± SD. Every symbol on graphs represents data obtained for individual WT (o) and MVI-KO (Δ) mice. In A, N=23 for WT and N=12 for MVI-KO P0 samples; N=13 for WT and N=11 for MVI-KO 3M samples; N=9 for WT and N=12 for MVI-KO 12M samples. In B, N=21 for WT and N=12 for MVI-KO P0 samples; N=11 for WT and N=10 for MVI-KO 3M samples; N=9 for WT and N=9 for MVI-KO 12M samples. In C, N=23 for WT and N=12 for MVI-KO P0 samples); N=12 for WT and N=11 for MVI-KO 3M samples); N=9 for WT and N=12 for MVI-KO 12M samples. In D, N=19 for WT and N=11 for MVI-KO P0 samples; N=9 for WT and N=10 for MVI-KO 3M samples); N=9 for WT and N=12 for MVI-KO 12M samples. Statistical significance was analyzed with t-test or one-way ANOVA test, *, $p<0.05$. One-way ANOVA with Tukey's multiple comparisons test was used for Fig. 1C. DF (degree of freedom), 43; F (F-statistics), 2,353.

Evaluation of MVI level

To reveal whether the content of MVI in the brain and its regions changes with the animal growth and maturation, we performed Western blot analysis of homogenates of P0, 3M, and 12M WT samples. As presented in Fig. 4A-D and Fig. 5A-D, the lowest MVI level was in newborns and the highest in samples of adult animals (3M and 12M). However, except the hippocampus, these differences were not statistically significant (Fig. 4D and Fig. 5D). Also, there was no significant difference between the level of MVI in the examined brain regions with respect to the total brain, irrespective of the animal age (Fig. 6).

Effects of lack of MVI on the level of gliosis markers

To understand the reported involvement of MVI in the development of gliosis (Osterweil et al., 2005), we performed immunoblotting for GFAP in the whole brain, cerebral cortex, cerebellum, and hippocampus samples of P0, 3M, and 12M WT and MVI-KO mice (Fig. 4A-D and 7A-D). The analysis revealed that in P0 animals, GFAP was not detectable in all the examined samples. However, in adult MVI-KO samples, the level of this protein was significantly higher than in WT samples. Furthermore, we assessed whether the GFAP level changes between 3M and 12 M WT and MVI-KO

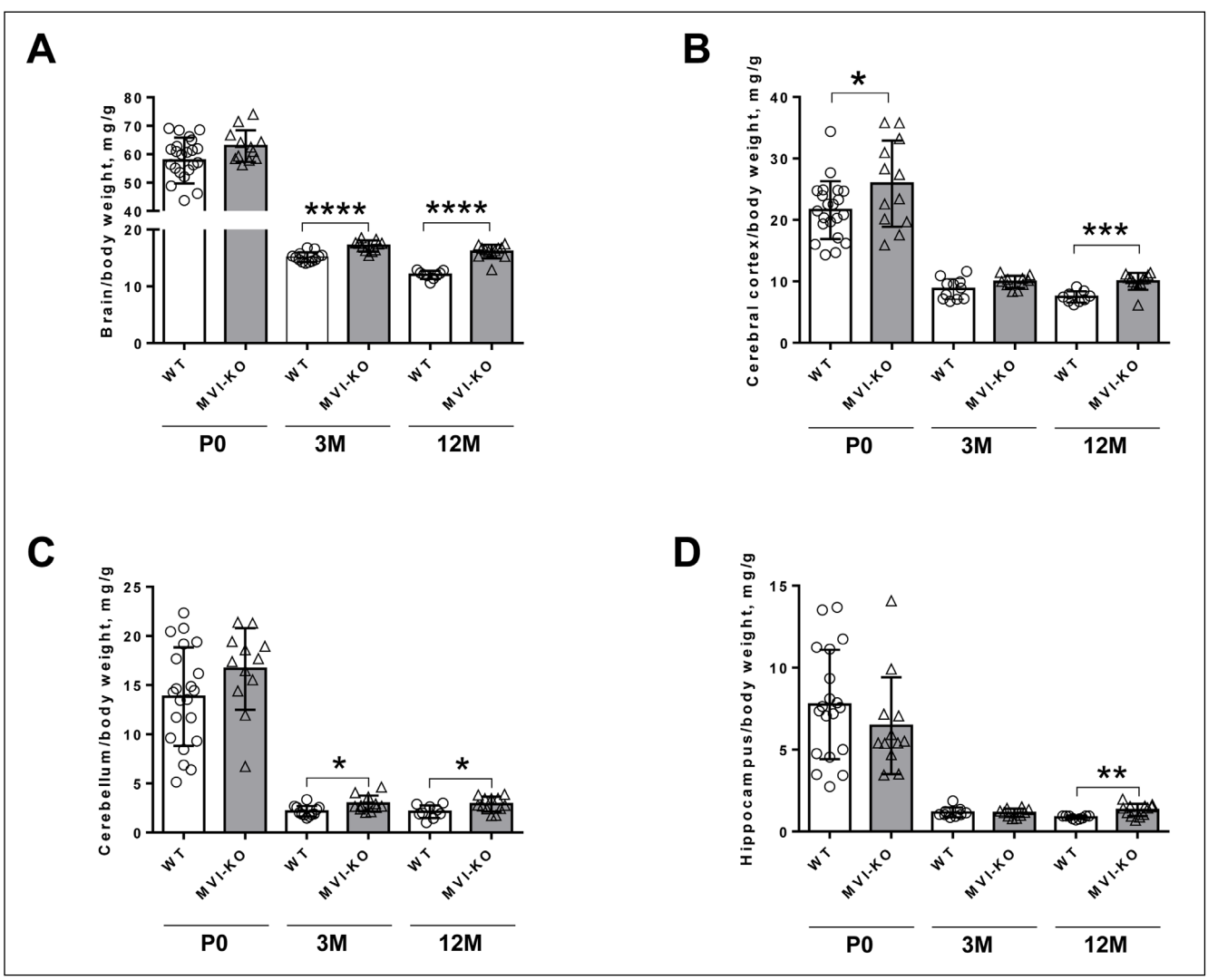

Fig. 2. Effect of lack of MVI on the brain- and its regions-to-body weight ratio. Evaluation of the ratios of the total brain- (A), cerebral cortex- (B), cerebellum- (C), and hippocampus- (D) to the body weight ratio in WT and MVI-KO P0, 3M and 12M mice was performed. The data are presented as mean ± SD. Every symbol on graphs represents data obtained for individual WT (o) and MVI-KO (Δ) mice. The N values as in Fig. 1. Statistical significance was analyzed with t-test or one-way ANOVA test, *, p<0.05, **, p<0.01, ***, p<0.001, ****, p<0.0001. One-way ANOVA with Tukey's multiple comparisons test was used for Fig. 2C. DF (degree of freedom), 43; F (F-statistics), 4,515.

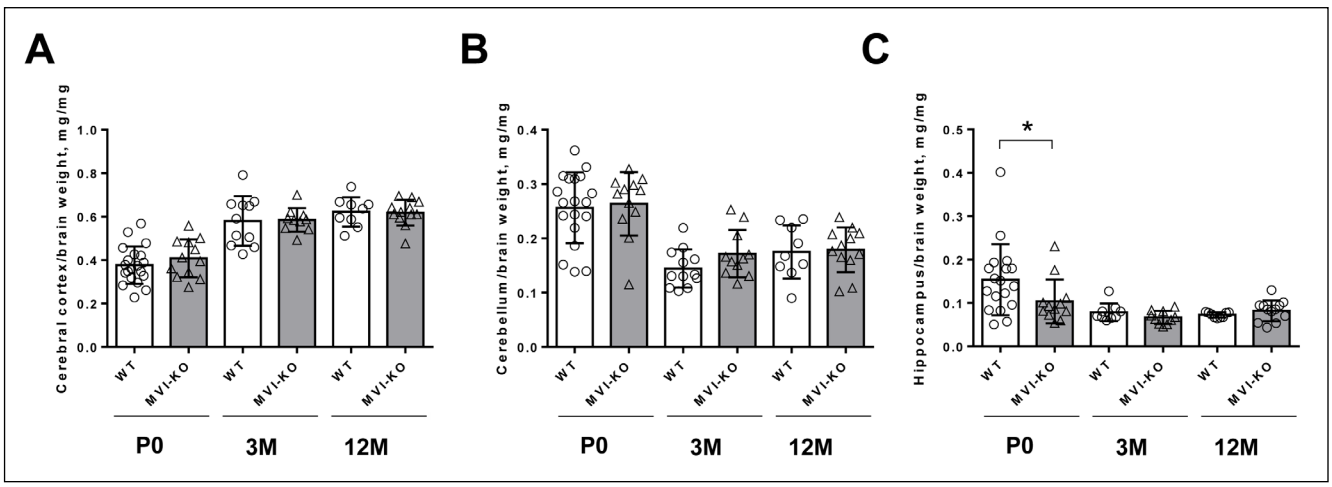

Fig. 3. Effect of lack of MVI on the ratio of brain regions weight to whole brain weight. Evaluation was performed for cerebral cortex (A), cerebellum (B), and hippocampus (C) of WT and MVI-KO P0, 3M and 12M mice. The data are presented as mean ± SD. Every symbol on graphs represents data obtained for individual WT (o) and MVI-KO (Δ) mice. The N values as in Fig. 1. Statistical significance was analyzed with t-test or one-way ANOVA test, *, $p<0.05$. One-way ANOVA with Tukey's multiple comparisons test was used for Fig. 3. A; DF (degree of freedom) 41, F (F-statistics) - 0,8098 and Fig. 3. B – DF (degree of freedom) 43, F (F-statistics) – 1,619.

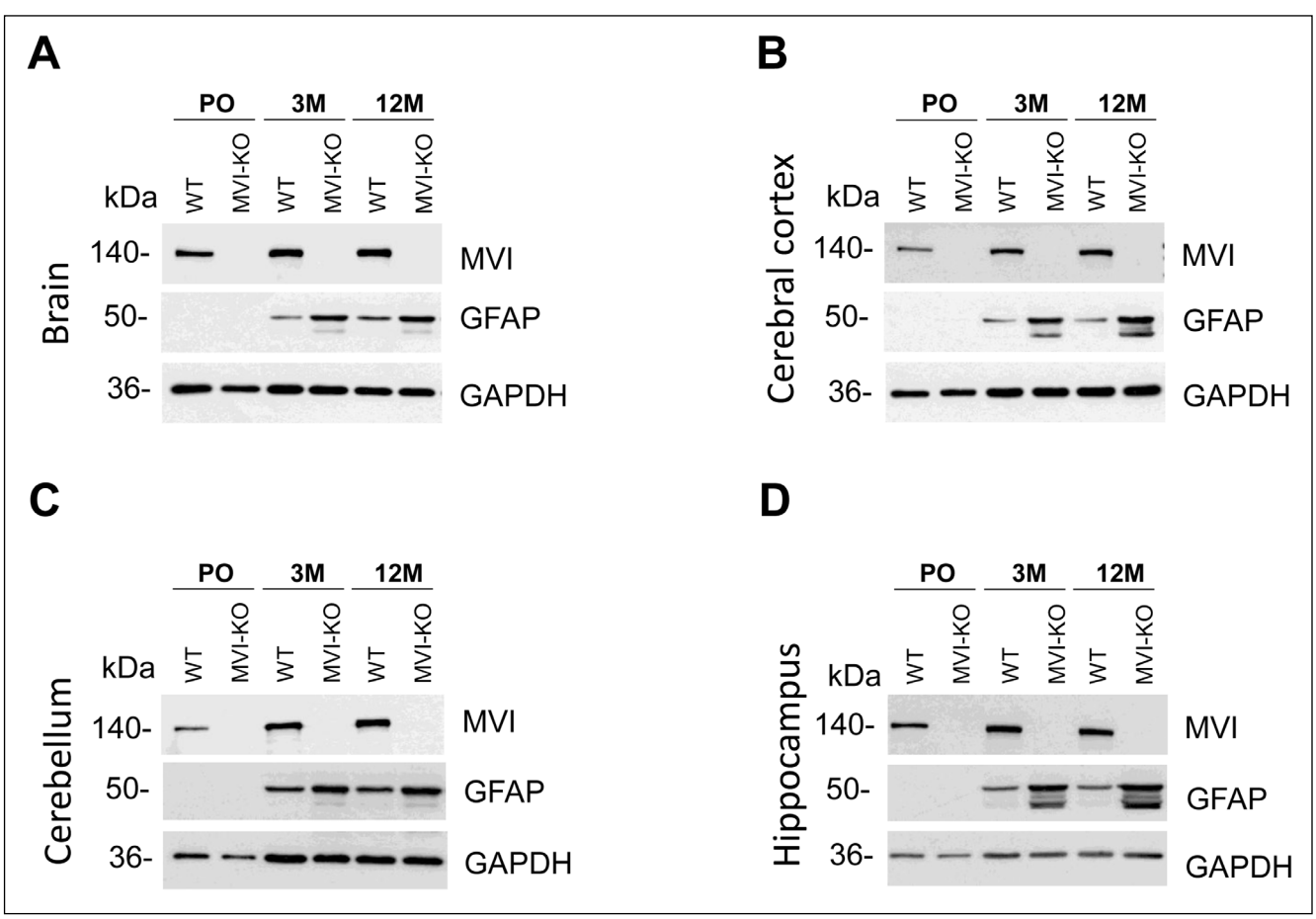

Fig. 4. Evaluation of MVI and GFAP levels in the brain and its regions of WT and MVI-KO mice. (A) total brain, (B) cerebral cortex, (C) cerebellum, (D) hippocampus. Immunoblotting analyses with the use of specific antibodies against MVI and GFAP were performed on the homogenates of WT and MVI-KO P0, 3M and 12M mice as described in Methods. GAPDH (glyceraldehyde-3-phosphate dehydrogenase) was used as the internal loading control. Densitometric analysis of the MVI level is presented in Fig. 5 and 6, and of GFAP in Fig. 7.

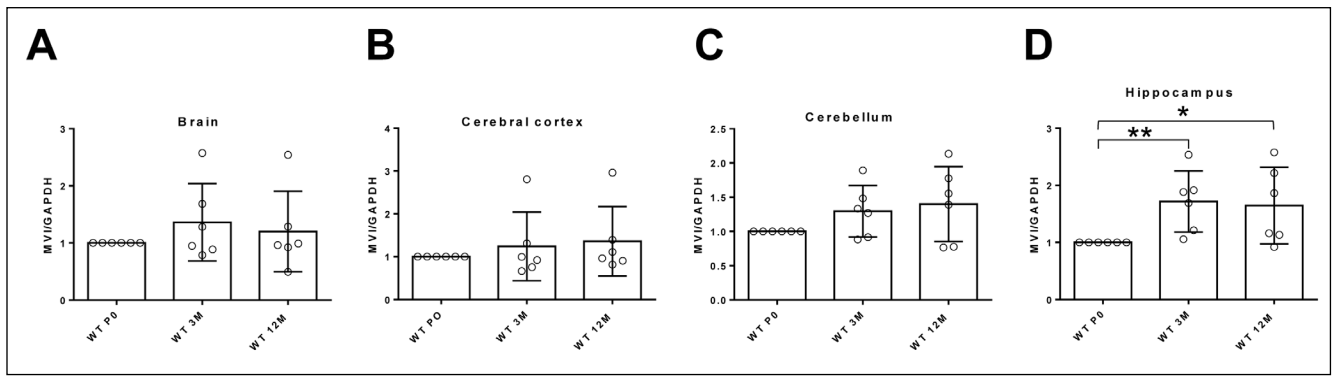

Fig. 5. Evaluation of MVI levels in the brain and its regions. (A) whole brain, (B) cerebral cortex, (C) cerebellum, (D) hippocampus. The densitometric analysis of immunoblots presented in Fig. 4 was performed as described in the Methods. The data are presented as mean ± SD, N=6 for each examined sample. Every symbol on graphs represents data obtained for individual WT (o). Statistical significance was analyzed with Kruskal-Wallis test, *, $p<0.05$, **, $p<0.01$. Values obtained for P0 samples served as 1. GAPDH was used as the internal loading control.

samples. While we observed a tendency of an increase of GFAP level in all the examined samples, the statistically significant changes were found only in the cerebral cortex and hippocampus of WT samples, as well as in the cerebellum of MVI-KO samples. Also, we detected additional bands with a higher electrophoretic mobility in 3M and 12M MVI-KO brains and its regions.

Additionally, to get more insight into the development of gliosis in P0 MVI-KO brains, we performed immunoblotting for an intermediate filament protein, vimentin, in the whole brain (Fig. 8A) and hippocampus (Fig. 8B). Densitometric analysis revealed that there is no difference between the MVI-KO and WT samples.

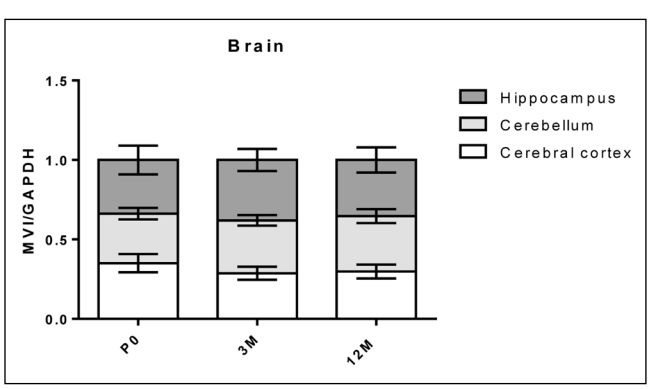

Fig. 6. Comparison of the MVI levels in the examined brain regions with respect to the whole brain level. The densitometric analyses of blots presented in Fig. 4 were performed on the homogenates of the whole brain, cerebral cortex, cerebellum and hippocampus of P0, 3M and 12M WT mice; 1 reflects the MVI level in the whole brain. The details are described in Methods. The data are presented as mean ± SEM, N=6 for each examined sample. No statistical significance was obtained.

DISCUSSION

We have addressed herein the role of MVI in the brain using samples of brains and its regions (i.e., cerebral cortex, cerebellum, and hippocampus) derived from P0, 3M, and 12 M mice lacking MVI (SV, MVI-KO) with respect to control heterozygous counterparts (WT).

Our data not only confirmed the MVI presence in the murine brains, but also showed that its level is increasing with age. We were the first to demonstrate this time-dependent MVI synthesis as it was only Osterweil et al. (2005), who addressed this issue and showed that *Myo6* expression in the whole mouse brain did not change from birth to early adulthood. However, the authors examined only brains isolated from day 1 to day 45 after birth. Moreover, their quantitative studies were performed on whole-brain samples, while we showed that the MVI level is increased in all examined brain regions, with the most evident difference observed for the hippocampus. This age-dependent increase of the MVI level is in contrast to our own observations on murine skeletal and cardiac muscles, where we showed that the MVI level is highest in newborns and decreases with age (Karatsai et al., 2023; Wojton et al., 2025).

We revealed that the increase in MVI level in adult brains coincides with the enlargement of the brain and its regions in MVI-KO animals, assessed as the ratio of the brain (and its examined regions) to the body weight. This correlation was most evident for brains of adult animals, where the differences between the examined ratios of WT and MVI-KO mice had the highest statistical significance with p values below 0.0001. These findings suggest that the lack of MVI evokes time-dependent changes in the brain structure and

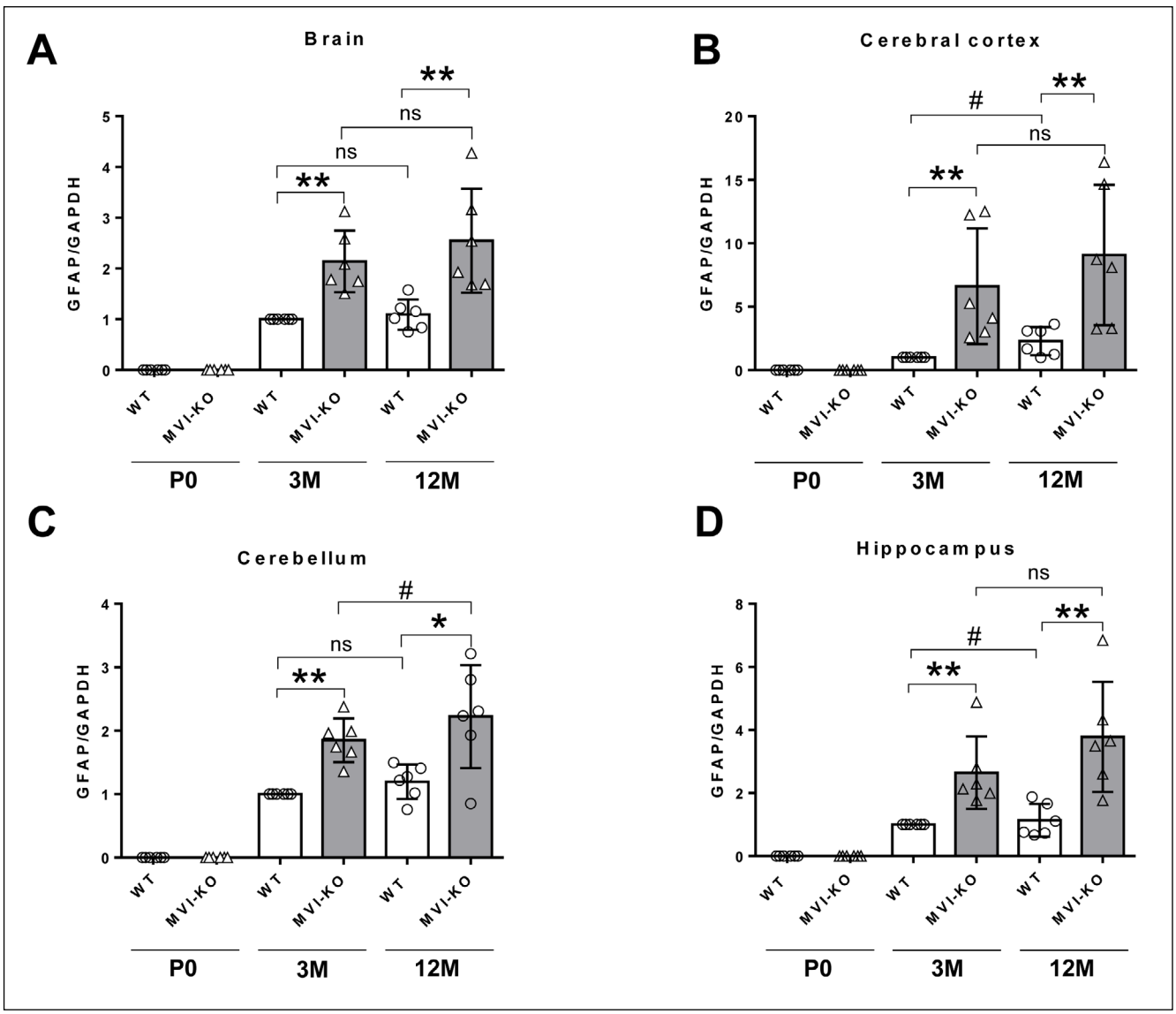

Fig. 7. Evaluation of GFAP levels in the brain and its regions. (A) total brain, (B) cerebral cortex, (C) cerebellum, (D) hippocampus. The analyses of immunoblots presented in Fig. 4 with the use of specific antibodies to MVI and GFAP were performed on the homogenates of WT and MVI-KO P0, 3M and 12M mice. The details are described in the Methods section. The data are presented as mean ± SD. Every symbol on graphs represents data obtained for individual WT (o) and MVI-KO (Δ) mice; N=6 for all samples. Statistical significance was analyzed with Mann-Whitney test. * or #, $p<0.05$. *, comparisons between MVI-KO and control WT counterparts at the indicated age, and #, comparisons between 3M and 12M WT or 3M and 12M MVI-KO animals, ns – no statistical significance. GAPDH was used as the internal loading control.

possibly function. However, so far, there are no reports addressing this problem. Our analysis also indicates that the abovementioned enlargement concerns in the brain regions to the same extent as the ratio of the weight of examined brain areas to the whole brain did not differ between WT and MVI-KO samples at all time points. It is noteworthy that we also found that in skeletal muscle and the heart a lack of MVI leads to hindlimb muscles (especially slow-twitch soleus) and heart enlargement but unlike in the brain, these differences were most prominent in MVI-KO newborns. We revealed that these differences resulted from fiber hyperplasia and/or increased proliferation during early stages of skeletal and cardiac muscle growth and development (Lehka et al., 2022; Karatsai et al., 2023).

It has been shown that the observed MVI-loss-associated brain enlargement is the effect of profound gliosis, which was assessed by examination of GFAP level and astrocyte staining (Osterweil et al., 2005). This excessive gliosis in adult brains is considered to be responsible for the observed impairment of neurotransmission (Yano et al., 2006; Nash et al., 2010;

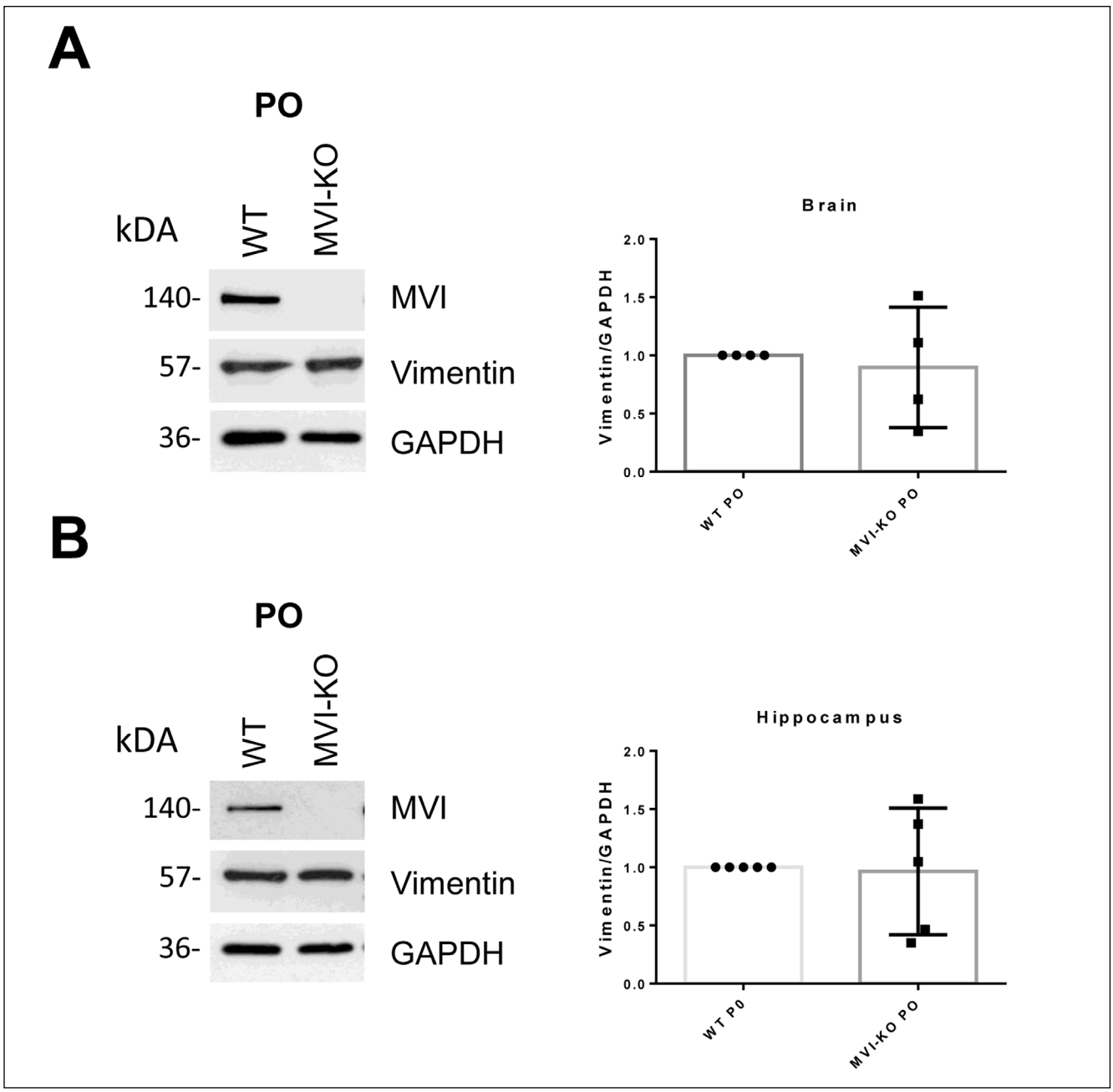

Fig. 8. Evaluation of vimentin levels in the whole brain (A) and hippocampus (B). In A and B, left panels, representative immunoblots, and in the right, densitometric analyses, which were performed on the homogenates of WT and MVI-KO P0 samples with the use of specific antibodies against vimentin. The details are described in the Methods. The data are presented as mean ± SD; statistical significance. N= 4 for all samples. Every symbol on graphs represents data obtained for individual WT (●) and MVI-KO (■) mice. Values obtained for WT samples served as 1. GAPDH was used as the internal loading control. No statistical significance was obtained.

Wagner et al., 2019). However, it is not known when MVI-loss-associated gliosis develops, as to our best knowledge, nobody has addressed this problem so far. Therefore, we evaluated the level of GFAP in all the examined samples. While we observed that the level of GFAP is increasing in the whole brains and examined areas between 3M and 12 M, both WT and MVI-KO mice (with the highest levels in 12M MVI-KO brains), we were not able to detect GFAP in newborn samples of both 3M and 12M samples. These observations seem to suggest that MVI-loss-dependent gliosis develops with age. However, these data may be interpreted as that in newborns the GFAP level is beyond the detection capability of the immunoblot-

ting technique, since it is known that in neonates the level of this gliosis marker is low, and increases with age (Chiu & Goldman, 1985). To verify whether the MVI-associated gliosis develops with age, we assessed in the whole brain and hippocampus homogenates of newborn mice for the level of vimentin, an intermediate filament protein, which is produced by proliferating microglia (Kreutzberg et al., 1989). Our observation that there was no difference between vimentin levels in WT and MVI-KO samples seems to indicate that there is no gliosis in newborns, confirming our suggestion that MVI-loss-dependent gliosis develops with animal growth and maturation. However, the question of how MVI contributes to this phenomenon remains a matter of dispute.

It is noteworthy that up-regulation of GFAP has been shown, among others, in stroke, epilepsy, or in neurodegenerative diseases (Little & O'Callagha, 2001; Mandybur, 1989), suggesting that excessive gliosis contributes to the observed decrease of synaptic activity in MVI-KO neurons (Osterweil et al., 2005; Yano et al., 2006; Hayashida et al., 2015; Wagner et al., 2019). Also, we observed the presence of additional GFAP bands, known to be the result of the increased caspase activity (Mouser et al., 2013). However, it is also known that in the pathological brains (upon injuries or with neurodegeneration, including Alzheimer's disease, AD) expression of other GFAP isoforms with a lower molecular weight is taking place (de Reus et al., 2024; Hol, 2024). Thus, these data seem to suggest a possible link between lack of MVI and AD development, which seem to be confirmed by the presence of a few reports addressing this issue (Tamaki et al., 2008; Feuillette et al., 2010; Bowirrat et al., 2010; Lee et al., 2024). For example, Feuillette et al. (2010) showed that MVI and filamin A (a protein involved in the actin cytoskeleton assembly) colocalize with fibrillary tau protein in several tauopathies such as AD, fronto-temporal dementia, Pick's disease, and progressive supranuclear palsy. Moreover, recently Lee et al. (2024) demonstrated that *Myo6* was hypermethylated in the hippocampus of an AD mouse model, leading to a decrease in its transcript level. Additionally, in line with the abovementioned observations are our preliminary data showing that the level of MVI was decreased in the temporal cortex of AD patients (not shown).

CONCLUSION

We showed for the first time that the lack of MVI leads to the age-dependent enlargement of the mouse brain and its regions, as well as in the development of profound gliosis.

ACKNOWLEDGMENTS

We thank Dr. Folma Buss from the Cambridge Institute for Medical Research, University of Cambridge, United Kingdom, for her gift of Snell's waltzer mice. Also, we appreciate the help of Dr. Olena Karatsai-Miąskowska in figure preparation. This work was supported by the statutory funds from the Ministry of Science and Higher Education to the Nencki Institute.

REFERENCES

Avraham, K. B., Hasson, T., Sobe, T., Balsara, B., Testa, J. R., Skvorak, A. B., Morton, C. C., Copeland, N. G., & Jenkins, N. A. (1997). Characterization of unconventional MYO6, the human homologue of the gene responsible for deafness in Snell's waltzer mice. Hum Mol Genet, 6, 1225–1231. https://doi: 10.1093/hmg/6.8.1225.

Berg, J. S., Powell, B. C., & Cheney, R. E. (2001). A millenial myosin census. Mol Biol Cell, 12, 780–794. https://doi: 10.1091/mbc.12.4.780.

Bowirrat, A., Chen, T. J. H., Blum, K., Madigan, M., Bailey, J. A., Chuan Chen, A. L., Downs, B. W., Braverman, E. R., Radi, S., Waite, R. L., Kerner, M., Giordano, J., Morse, S., Oscar-Berman, M., & Gold, M. (2010). Neuro-psychopharmacogenetics and neurological antecedents of post-traumatic stress disorder: unlocking the mysteries of resilience and vulnerability. Curr Neuropharmacol, 8(4), 335–358. https://doi: 10.2174/157015910793358123.

Chibalina, M. V., Puri, C., Kendrick-Jones, J., & Buss, F. (2009) Potential roles of myosin VI in cell motility. Biochem. Soc. Trans, 37, 966–970. https://doi: 10.1042/BST0370966.

de Reus, A. J. E. M., Basak, O., Dykstra, W., van Asperen, J. V., van Bodegraven, E. J., & Hol, E. M. (2024). GFAP-isoforms in the nervous system: Understanding the need for diversity. Current opinion in cell biology, 87, 102340. https://doi.org/10.1016/j.ceb.2024.102340?

Chiu, F.C. & Goldman, J.E. (1985) Regulation of glial fibrillary acidic protein (GFAP) expression in CNS development and in pathological states. J Neuroimmunol, 8, 283–292. https://doi: 10.1016/s0165-5728(85)80067-9.

Hol, E. M. (2024). GFAP-isoforms in the nervous system: Understanding the need for diversity. Curr Opin Cell Biol, 87, 102340. https://doi: 10.1016/j.ceb.2024.102340.

Deng, C., Moradi, M., Reinhard, S., Ji, C., Jablonka, S., Hennlein, L., Lüningschrör, P., Doose, S., Sauer, M., & Sendtner, M. (2021). Dynamic remodeling of ribosomes and endoplasmic reticulum in axon terminals of motoneurons. J Cell Sci, 134(22), jcs258785. https://doi: 10.1242/jcs.258785.

Deol, M. S., & Green, M. C. (1966). Snell's waltzer, a new mutation affecting behaviour and the inner ear in the mouse. Genet Res, 18(3), 339–345. https://doi: 10.1017/s0016672300010193.

Feuillette, S., Deramecourt, V., Laquerriere, A., Duyckaerts, C., Delisle, M. B., Maurage, C A., Blum, D., Buée, L., Frébourg, T., Campion, D., & Lecourtois, M. (2010). Filamin-A and Myosin VI colocalize with fibrillary Tau protein in Alzheimer's disease and FTDP-17 brains. Brain Res, 1345, 182–189. https://doi: 10.1016/j.brainres.2010.05.007.

Hari-Gupta, Y., Fili, N., Dos Santos, Á., Cook, A. W., Gough, R. E., Reed, H. C. W., Wang, L., Aaron, J., Venit, T., Wait, E., Grosse-Berkenbusch, A., Gebhardt, J. C. M., Percipalle, P., Chew, T. L., Martin-Fernandez, M., & Toseland, C. P. (2022). Myosin VI regulates the spatial organisation of mammalian transcription initiation. Nat Commun, 13, 1346. https://doi: 10.1038/s41467-022-28962-w.

Hayashida, M., Tanifuji, S., Ma, H., Murakami, N., & Mochida, S. (2015). Neural activity selects myosin IIB and VI with a specific time window in dis-

tinct dynamin isoform-mediated synaptic vesicle reuse pathways. J Neurosci, 35(23), 8901–8913. https://doi: 0.1523/JNEUROSCI.5028-14.2015.

Karatsai, O., Lehka, L., Wojton, D., Grabowska, A. I., Duda, M. K., Lenartowski, R., & Redowicz, M. J. (2023) Unconventional myosin VI in the heart: involvement in cardiac dysfunction progressing with age. Biochim Biophys Acta Mol Basis Dis, 1869, 166748. https://doi: 10.1016/j.bbadis.2023.166748.

Karolczak, J., Sobczak, M., Majewski, L., Yeghiazaryan, M., Jakubiec-Puka, A., Ehler, E., Sławinska, U., Wilczyński, G. M., & Rędowicz, M. J. (2013). Myosin VI in skeletal muscle: its localization in the sarcoplasmic reticulum, neuromuscular junction and muscle nuclei. Histochem Cell Biol 139, 873–885. https://doi: 10.1007/s00418-012-1070-9.

Kreutzberg, G. W., Graeber, M. B., Streit, W. J. (1989). Neuron-glial relationship during regeneration of motoneurons. Metab Brain Dis, 4(1), 81–85. https://doi: 10.1007/BF00999498.

Kruppa, A. J., Kishi-Itakura, C., Masters, T. A., Rorbach, J. E., Grice, G. L., Kendrick-Jones, J., Nathan, J. A., Minczuk, M., & Buss, F. (2018). Myosin VI-dependent actin cages encapsulate Parkin-positive damaged mitochondria. Dev Cell, 44, 484–499.e6. https://doi: 10.1016/j.devcel.2018.01.007.

Lee, S., Lee, H. J., Mi Chun, J., Jung, B., Kim, J., Moon, C., Kim, C., & Kim J. S. (2024). Integrated genome-wide analysis of DNA methylation and gene expression in the hippocampi of 5xFAD Alzheimer's disease mouse model. J Neurobiol, 42(3), 370–382. https://doi: 10.31083/j.jin2307138.

Lehka, L., Wojton, D., Topolewska, M., Chumak, V., Majewski, Ł., & Rędowicz, M. J. (2022). Lack of unconventional myosin VI affects cAMP/PKA signaling in hindlimb skeletal muscle in an age-dependent manner. Front Physiol, 13, 933963. https://doi: 10.3389/fphys.2022.933963.

Lewis, T. L., Mao, T., & Arnold, D. B. (2011). A role for myosin VI in the localization of axonal proteins. PLoS Biology, 9(3), e1001021. https://doi: 10.1371/journal.pbio.1001021.

Little, A. R., & O'Callagha, J. P. (2001). Astrogliosis in the adult and developing CNS: is there a role for proinflammatory cytokines? Neurotoxicology, 22(5), 607–618. https://doi: 10.1016/s0161-813x(01)00032-8.

Magistrati, E., & Polo, S. (2021). Myomics: myosin VI structural and functional plasticity. Curr Opin Struct Biol, 67, 33–40. https://doi: 10.1016/j.sbi.2020.09.005.

Majewski, Ł., Sobczak, M., Havrylov, S., Jóźwiak, J., & Rędowicz, M. J. (2012). Dock7: a GEF for Rho-family GTPases and a novel myosin VI-binding partner in neuronal PC12 cells. Biochem Cell Biol, 90(4), 565–574. https://doi: 10.1139/o2012-009.

Makioka, K., Yamazaki, T., Takatama, M., Ikeda, M., Murayama, S., Okamoto, K., & Ikeda, Y. (2016). Immunolocalization of Tom1 in relation to protein degradation systems in Alzheimer's disease. J Neurol Sci, 365, 101–107. https://doi: 10.1016/j.jns.2016.03.035.

Mandybur, T. I. (1989). Cerebral amyloid angiopathy and astrocytic gliosis in Alzheimer's disease. Acta Neuropathol, 78, 329–331. https://doi: 10.1007/BF00687764.

Mouser, P.E., Head, E., Ha, K.H., & Rohn T.T. (2006). Caspase-mediated cleavage of glial fibrillary acidic protein within degenerating astrocytes of the Alzheimer's disease brain. Am J Pathol, 168, 936–946. https://doi: 10.2353/ajpath.2006.050798.

Nash, J. E., Appleby, V. J., Corrêa, S. A. L., Wu, H., Fitzjohn, S. M., Garner, C. C., Collingridge, G. L., & Molnár, E. (2010). Disruption of the interaction between myosin VI and SAP97 is associated with a reduction in the number of AMPARs at hippocampal synapses. J Neurochem, 112(3), 677–690. https://doi: 10.1111/j.1471-4159.2009.06480.x.

Nishikawa, S., Homma, K., Komori, Y., Iwaki, M., Wazawa, T., Hikikoshi Iwane, A., Saito, J., Ikebe, R., Katayama, E., Yanagida, T., & Ikebe, M. (2002) Class VI myosin moves processively along actin filaments backward with large steps. Biochem Biophys Res Commun, 290, 311–317. https://doi: 10.1006/bbrc.2001.6142.

Nowak, J., Lenartowski, R., Kalita, K., Lehka, L., Karatsai, O., Lenartowska, M., & Rędowicz, M. J. (2024). Myosin VI in the nucleolus of neurosecretory PC12 cells: its involvement in the maintenance of nucleolar structure and ribosome organization. Front Physiol, 15, 1368416. https://doi: 10.3389/fphys.2024.1368416.

Odronitz, F., & Kollmar, M. (2007). Drawing the tree of eukaryotic life based on the analysis of 2,269 manually annotated myosins from 328 species. Genome Biol, 8(9), R196. https://doi: 10.1186/gb-2007-8-9-r196.

Osterweil, E., Wells, D. G., & Mooseker, M. S. (2005). A role for myosin VI in postsynaptic structure and glutamate receptor endocytosis. J Cell Biol, 168, 329–338. https://doi: 10.1083/jcb.200410091.

Redowicz, M. J. (2002). Myosins and pathology: genetics and biology. Acta Biochim Pol, 49, 789–804.

Sundaramoorthy, V., Walker, A. K., Tan, V., Fifita, J. A., Mccann, E. P., Williams, K. L., Blair, I. P., Guillemin, G. J., Farg, M. A., & Atkin, J. D. (2015). Defects in optineurin- and myosin VI-mediated cellular trafficking in amyotrophic lateral sclerosis. Hum Mol Genet, 24(13), 3830–3846. https://doi: 10.1093/hmg/ddv126.

Suter, D. M., Espindola, F. S., Lin, C. H., Forscher, P., & Mooseker, M. S. (2000). Localization of unconventional myosins V and VI in neuronal growth cones. J Neurobiol, 42, 370–382.

Sweeney, H. L., & Houdusse, A. (2007). What can myosin VI do in cells? Curr Opinion Cell Biol, 19, 57–66. https://doi: 10.1016/j.ceb.2006.12.005.

Sweeney, H. L., & Houdusse, A. (2010). Myosin VI rewrites the rules for myosin motors. Cell, 141, 573–582. https://doi: 10.1016/j.cell.2010.04.028.

Takarada, T., Tamaki, K., Takumi T., Ogura, M., Ito, Y., Nakamichi, N., & Yoneda, Y. (2009). A protein-protein interaction of stress-responsive myosin VI endowed to inhibit neural progenitor self-replication with RNA binding protein, TLS, in murine hippocampus. Comparative Study J Neurochem, 110(5), 1457–1468. https://doi: 10.1111/j.1471-4159.2009.06225.x.

Tamaki, K., Kamakura, M., Nakamichi, N., Taniura, H., & Yoneda, Y. (2008). Upregulation of Myo6 expression after traumatic stress in mouse hippocampus. Neurosci Lett, 433(3), 183–187. https://doi: 10.1016/j.neulet.2007.12.062.

Wagner, W., Lippmann, K., Heisler, F. F., Gromova, K. V., Lombino, F. L., Roesler, M. K., Pechmann, Y., Hornig, S., Schweizer, M., Polo, S., Schwarz, J. R., Eilers, J., & Kneussel, M. (2019) Myosin VI drives clathrin-mediated AMPA receptor endocytosis to facilitate cerebellar long-term depression. Cell Rep;28(1): 11–20.e9. https://doi: 10.1016/j.celrep.2019.06.005.

Wells, A. L., Lin, A. W., Chen, L. Q., Safer, D., Cain., S. M., Hasson, T., Carragher, B. O., Milligan, R. A., & Sweeney, H. L. (1999). Myosin VI is an actin-based motor that moves backwards. Nature, 401, 505–508. https://doi: 10.1038/46835.

Wojton, D., Dymkowska, D., Matysniak, D., Topolewska, M., Redowicz, M. J., & Lehka, L. (2025) Unconventional myosin VI is involved in the regulation of muscle energy metabolism. American Journal of Physiology – Cell Physiology, 1, 329(4), C1004-C1021. https://doi: 10.1152/ajpcell.00300.2025.

Wu, H., Nash, J. E., Zamorano, P., & Garner, C. C. (2002). Interaction of SAP97 with minus-end directed actin motor protein myosin VI: implications for AMPA receptor trafficking. J Biol Chem, 277, 30928–30934. https://doi: 10.1074/jbc.M203735200.

Yano, H., Ninan, I., Zhang, H., Milner, T. A., Arancio, O., & Chao, M. V. (2006). BDNF-mediated neurotransmission relies on upon a myosin VI motor complex. Nature Neurosci 9, 1009–1018. https://doi: 10.1038/nn1730.

Yoong, L. F., Lim, H. K., Tran, H., , Lackner, S., Zheng, Z., Hong, P., & Moore, A. W. (2020). Atypical Myosin Tunes Dendrite Arbor Subdivision. Neuron, 106(3), 452–467.e8. https://doi: 10.1016/j.neuron.2020.02.002.

Zheng, P., Liu, Y., Chen, J., & Teng, J. (2015). Trip6 promotes dendritic morphogenesis through dephosphorylated GRIP1-dependent myosin VI and F-actin organization J Neurosci, 35(6), 2559–2571. https://doi: 10.1523/JNEUROSCI.2125-14.2015.